Kinetic evidence for the formation of a Michaelis–Menten-like complex between horseradish peroxidase compound II and di-(*N*-acetyl-L-tyrosine)

Weichi WANG*, Stéphanie NOËL†, Michel DESMADRIL‡, Jacques GUÉGUEN† and Thierry MICHON§[1]

*Department of Cellular and Molecular Pharmacology, University of California San Francisco, Box 0450, San Francisco, CA 94143-0448, U.S.A., †Unité de Biochimie et de Technologie des Protéines, INRA, rue de la Géraudière, BP 1627, 44316 Nantes, France, ‡EPCM, Bat. 430, Université Paris Sud, 91405 Orsay Cedex, France, and §Division of Chemistry and Chemical Engineering 210-41, California Institute of Technology, Pasadena, CA 91125, U.S.A.

The formation of a reversible adsorption complex between a dimer of *N*-acetyl-L-tyrosine [di-(*N*-acetyl-L-tyrosine), $(NAT)_2$] and horseradish peroxidase (HRP) compound II (C_{II}) was demonstrated using a kinetic approach. A specific K_m^{II} value (0.58 mM) was deduced for this step from stopped-flow measurements. The dimerization of the dipeptide Gly-Tyr was analysed at the steady state and compared with $(NAT)_2$ dimerization [$(NAT)_2 \rightarrow (NAT)_4$]. A saturation of the enzyme was observed for both substrates within their range of solubility. In each case the rate of dimerization reflected the rate-limiting step of compound II reduction to the native HRP (E) ($k_{cat}^{app}/K_m^{app} \approx k_{II \rightarrow E}$). The k_{cat}^{app} values for $(Gly\text{-}Tyr)_2$ and $(NAT)_4$ formation were 254 s^{-1} and 3.6 s^{-1} respectively. The K_M^{app} value of Gly-Tyr was 24 mM. It was observed that the value (0.7 mM) for $(NAT)_2$ was close both to its specific K_m^{II} value for the second step of reduction ($C_{II} \rightarrow E$) and to its thermodynamic dissociation constant ($K_d = 0.7$ mM) with the resting form of the enzyme. As $(NAT)_2$ was a tighter ligand but a poorer substrate than Gly-Tyr, a steady-state kinetic study was performed in the presence of both substrates. A kinetic model which includes an enzyme–substrate adsorption prior to each of the two steps of reduction was derived. This one agreed reasonably well with the experimental data.

Key words: di-tyrosine, K_m, peroxidase, substrate complex, saturation.

INTRODUCTION

The kinetic features of horseradish peroxidase (HRP) have been extensively investigated. The general mechanism of this oxidoreductase involves its oxidation by H_2O_2, followed by its two-step reduction mediated via two consecutive one-electron oxidations of donor substrates. The classic Chance model [1] does not involve any kind of Michaelis–Menten intermediate. This one agrees with experimental observations under most conditions [2]. For this reason the peroxidase cycle is generally considered as irreversible [3]. However, there is no doubt that adsorption complexes between the enzyme and its substrates physically exist. Previous studies have demonstrated that donors can bind to the enzyme in the absence of peroxide in the medium, and thermodynamic equilibrium constants were determined for several aromatic donors [4–6]. Microscopic constants governing the equilibrium between benzohydroxamic acid and HRP, either free or complexed with the cyanide iron ligand, were also estimated [7]. That study confirmed that even if the presence of one of the co-substrates (donor or H_2O_2) in the enzyme modulates the affinity for the other, the mechanism may proceed via random binding. This finding, together with some special kinetic features [8], support the notion that there is no need for the peroxide to bind to the enzyme prior to donor adsorption. Phenols are efficiently oxidized by peroxidases. Extremely reactive free radicals are released from the enzyme and condense spontaneously giving rise to polymers. Steady-state analysis of aromatic compound oxidation catalysed by HRP usually does not produce a classic Michaelis–Menten behaviour. One reason is that, upon oxidation, phenolic substrates give rise to complex mixtures of polymers with no defined stoichiometry of reaction. Moreover, very few substrates are able to saturate the enzyme within their domain of solubility. However, it is possible to observe a saturation of the enzyme in organic media, where aromatic substrates are better solubilized [9,10]. Finally the rates of oxidation of some substrates are so high that they cannot be determined accurately, even at very low substrate concentration. To our knowledge, little direct kinetic evidence for the formation of an adsorption complex between the HRP and one of its substrates has been reported so far. However it was previously observed that, at alkaline pH, H_2O_2 binds reversibly to the enzyme prior to HRP compound I (C_I) formation [11]. Critchlow and Dunford have also reported the formation of a complex between compound II and *p*-cresol at alkaline pH [12].

In vivo, peroxidases catalyse the polymerization of peptides and proteins through tyrosine condensation [13]. In a previous study we showed that HRP could be saturated by some tyrosine-containing peptides and, for this reason, an adsorption complex between the enzyme and substrate was postulated. Moreover, dimers formed in the early part of the reaction behaved like competitive inhibitors towards further oxidation of the monomers. A simple, albeit incomplete, model was developed which took into account the data obtained, including the fact that the dimers formed can also be oxidized by the enzyme. We demonstrated that the rate of dimerization determined at the steady state was consistent with the value of the microscopic rate constant corresponding to the reduction of the compound II (C_{II}) form of HRP to the resting enzyme. As this step was rate-limiting, it was the only one included in the model [14]. We also showed that di-(*N*-acetyl-L-tyrosine) [$(NAT)_2$], the dimeric form of *N*-acetyl-L-tyrosine, was a tighter ligand, but a poorer substrate, for compound II than was Gly-Tyr. In the work reported here, this dimer was used as a probe to demonstrate that a Michaelis–Menten like complex occurs between the oxidized

Abbreviations used: NAT, *N*-acetyl-L-tyrosine; $(NAT)_2$, di-(*N*-acetyl-L-tyrosine); C_{II}, horseradish peroxidase (HRP) compound II; C_I, HRP compound I; E, resting HRP; L-dopa, L-dihydroxyphenylalanine; BHA, benzohydroxamic acid.

[1] To whom correspondence should be addressed (e-mail michon@caltech.edu).

© 1999 Biochemical Society

forms of the enzyme (at least compound II) and the donor during the catalytic cycle of HRP.

MATERIALS AND METHODS

Enzymes

HRP (Type VI), was purchased from Sigma and used without further purification [R_z (Reinheitszahl ratio, A_{406}/A_{280}) 3.7 mean value].

Chemicals

N-Acetyl-L-tyrosine (NAT) and H_2O_2 were purchased from Sigma. Trifluoroacetic acid (Sequenal grade), acetonitrile (HPLC grade), sodium phosphate and potassium phosphate were obtained from Merck and were of the best grade available. Distilled water was further purified using a Milli-Q Millipore system. All buffers and solutions were filtered through a 0.22-μm-pore-size membrane before use.

Purification of $(NAT)_2$

The procedure for $(Tyr)_2$ preparation previously developed [15] proved to be transposable to $(NAT)_2$ preparation. All the samples were further purified by HPLC and characterized by MS before use [14].

Steady-state kinetics of dimerization

As in the case of tyrosine, the UV spectrum of tyrosine dimer displays a red shift upon ionization of the phenolic function. We found that the ionization of the $(Tyr)_2$ aromatic phenol exhibits a single pK_a value of 7.49. This finding confirmed the results previously reported [13]. All the experiments were performed at pH 8.7. At this pH value most of the dimer is ionized, while monomers are still protonated (the phenolic pK_a value for NAT being 9.86 according to our determination). Under such conditions the maximum of absorbance of the dimer occurs at 317 nm and the contribution of the monomer absorbance at this wavelength is negligible. Consequently the kinetics of dimerization were monitored through an increase of absorbance at 317 nm. This increase was linear for at least 1 min. allowing the determination of initial rates (v_0). The reaction mixture contained 2–10 nM HRP, 100 μM H_2O_2 and donors at various concentrations in 50 mM sodium phosphate, pH 8.7, at 37 °C. It was previously shown that the dimers formed in the early part of the reaction could in turn contribute to the reduction of the enzyme, giving rise to polymers of higher degree [14]. Tyrosine derivatives were allowed to react for 10–180 s, and the polymers obtained were separated by HPLC. Using their specific fluorescence properties (maximum emission at 407 nm) it was possible to detect very low amounts of polymers. After 3 min, the amount of $(NAT)_6$ and $(Gly\text{-}Tyr)_3$ (MS identification) in the mixture were 3 and 10 % of the total polymers starting from 1 mM $(NAT)_2$ and 30 mM Gly-Tyr respectively. As over this range of substrate concentrations the increase in absorbance was no longer linear, after 1 min it was assumed that, during the linear increase used for v_0 determination, the main contribution to the signal came from $(NAT)_4$ and $(Gly\text{-}Tyr)_2$.

Fast kinetic measurements

The measurements were performed using a three-syringe SFM3 stopped-flow device (Biologic, Grenoble, France). HRP and H_2O_2 were first mixed at equimolar concentrations (5–10 μM). Various amounts of a concentrated donor solution were added to the enzyme/peroxide pre-mix. The two-step reduction of the oxidized form of the enzyme (C_I) was monitored by the variations of absorbance at 422 nm. The acquisition time was set between 50 and 500 ms for C_I-to-C_{II} reduction and between 200 ms and 20 s for C_{II}-to-E reduction.

Spectrophotometric titration

Upon donor binding the spectrum of the resting HRP is slightly modified in the Soret region [16]. A decrease in absorbance (minimum effect at 375 nm and maximum effect at 403 nm) proportional to the amount of donor added was observed. Variations of absorbance $A_{403-375}$ were recorded for ligand concentrations ranging from 100 μM to 50 mM in the presence of 7 μM native HRP. In such conditions the free ligand concentration was close to the total ligand concentration ($[L]_{tot}$). Assuming one binding site on the enzyme, the following equation was used to fit the experimental data:

$$\Delta A = \Delta A_{max}[L]_{tot}/K_d + [L]_{tot} \quad (1)$$

with ΔA and ΔA_{max} being the variation in absorbance for a given ligand concentration and at ligand saturation respectively.

Adjustment of the kinetic parameters to the experimental data

Data fitting was obtained by mean of non-linear regression using the Marquardt–Levenburg algorithm [17]. For data fitting to the general model (eqn. 3 in the Results and discussion section), starting estimates of α_1, β_1, α_2 and β_2 were obtained from a pre-fit of the experimental initial rates (v_0) to the model using the Simplex graphical method [18].

RESULTS AND DISCUSSION

Steady-state kinetic parameters for the oxidation of $(NAT)_2$ and Gly-Tyr

A saturation of the enzyme was observed for both substrates (Figure 1) within their range of solubility. When the experiments were performed with $(NAT)_2$, the signal-to-noise ratio decreased as the concentration of substrate increased. This was due to the fact that the substrate, $(NAT)_2$, and the product of its self-condensation, $(NAT)_4$, both display high molar absorption coefficients at 317 nm, the wavelength used to monitor the dimerization. For this reason it was not possible to perform accurate measurements for concentrations of $(NAT)_2$ above 1.5 mM. The experimental data were fitted to the following equation (this is eqn. A39 in the Appendix divided by a factor of 2, as here v_0 represents the initial rate of dimer formation):

$$\frac{v_0}{[E]_0} = \frac{k'_1 k^{app}_{cat_{[A]}}}{(k'_1 + k^{app}_{cat_{[A]}})} \times \frac{[A]}{K^{app}_{M_{[A]}} \dfrac{k'_1}{(k'_1 + k^{app}_{cat_{[A]}})} + [A]} \quad (2)$$

with $k'_1 = k_1\ [H_2O_2]$ and [A] being the donor concentration [$(NAT)_2$ or Gly-Tyr in the present study].

The kinetic parameters k^{app}_{cat} and K^{app}_m were corrected from the expression $k_1[H_2O_2]$, a term referring to the formation of C_I starting from H_2O_2 and the resting enzyme. The value of k_1 (1.8×10^7 $M^{-1} \cdot s^{-1}$) was obtained from stopped-flow measurements, as previously described [11]. After corrections the values of k^{app}_{cat} were 254 ± 12 s^{-1} and 3.6 ± 0.1 s^{-1} for Gly-Tyr and $(NAT)_2$ respectively. The values of K^{app}_m were 24 ± 2 mM and 0.66 ± 0.05 mM for Gly-Tyr and $(NAT)_2$ respectively. In a previous study, it was found that $(NAT)_2$, owing both to its low rate of oxidation and to its high affinity for HRP, could behave as a competitive-like inhibitor of the oxidation of other tyrosine-

© 1999 Biochemical Society

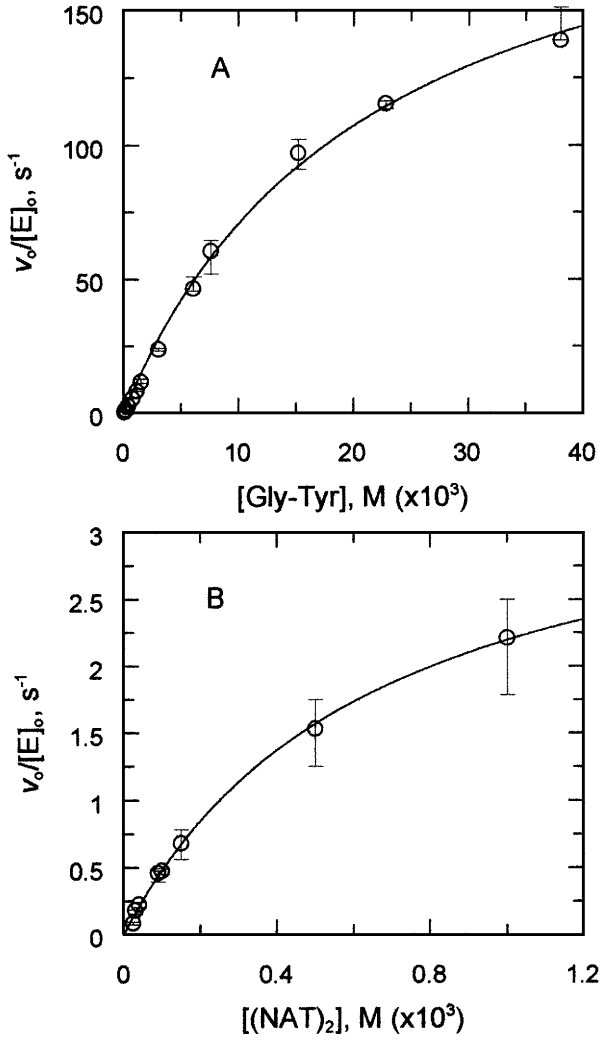

Figure 1 Steady-state kinetics of tyrosine-compound dimerization following oxidation by HRP

Reactions were performed in the presence of 4 nM HRP and 100 μM H_2O_2 at 37 °C in 50 mM sodium phosphate, pH 8.7. Continuous lines represent theoretical curves calculated using kinetic parameters corresponding to the best fit of the experimental values to eqn. (2).

containing substrates. Its apparent dissociation constant with the enzyme ($K_I^{app} \approx 20\ \mu$M) was indirectly evaluated using a steady-state kinetic test. Because of its low rate of oxidation $(NAT)_2$ was considered as a strict competitive inhibitor. Consequently the steps involving the oxidation of $(NAT)_2$ were not taken into account in our previous model [14]. As seen above, this led to an underestimation of its dissociation constant with the enzyme.

Steady-state kinetics of Gly-Tyr dimerization in the presence of finite concentrations of $(NAT)_2$

The kinetic of dimerization of Gly-Tyr was slowed down in the presence of $(NAT)_2$ (Figure 2A). Hanes plots [19] of the initial rate of dimerization, v_0, in the presence of finite concentrations of $(NAT)_2$ showed that, albeit saturation was achieved, this was not a simple 'Michaelian' kinetic (Figure 2B). For concentrations of Gly-Tyr below 500 μM, the kinetic was not pseudo-first-order. Over this range of substrate concentrations the mixture contained three species of polymers absorbing at the wavelength used for measurements. These polymers, namely $(Gly\text{-}Tyr)_2$, $(NAT)_4$ and Gly-Tyr-$(NAT)_2$, display different molar absorption coefficients. The ΔA_{317} observed was the sum of the contribution of all these species. This led to an overestimation of the rate. Since it was not possible to determine easily the proportion of the different molecules in the mixture, all the rates measured in this range of Gly-Tyr concentrations were discarded for further analysis. We derived a kinetic model making allowance for (i) the oxidation of HRP to C_I ($E \rightarrow C_I$); (ii) the two steps of reduction of C_I to E ($C_I \rightarrow C_{II} \rightarrow E$); (iii) the presence of two different substrates simultaneously in the medium [A = Gly-Tyr and B = $(NAT)_2$]; (iv) reversible steps of association between C_I and A or B and between C_{II} and A or B. This model is schematized as follows:

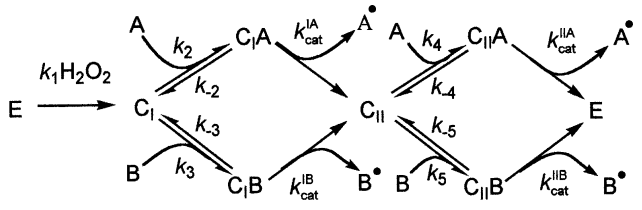

Scheme 1

The equation of the initial rate of formation of free radicals corresponding to this Scheme is:

$$\frac{v_0}{[E]_0} = 2 \times \frac{[A]^2 + \beta_1[A] + \beta_2}{\left(\frac{1}{k_{cat}^{A}} + \frac{1}{k_1[H_2O_2]}\right)[A]^2 + \left(\alpha_1 + \frac{\beta_1}{k_1[H_2O_2]}\right)[A] + \left(\alpha_2 + \frac{\beta_2}{k_1[H_2O_2]}\right)} \quad (3)$$

It is derived in the Appendix as eqn. (A30). α_1, α_2, β_1 and β_2 are functions of $(NAT)_2$ concentration and of the kinetic parameters which describe the system. For Gly-Tyr concentrations above 500 μM the experimental data were fitted to the model (Figure 2A) as the mean product of oxidation present in the mixture becomes $(Gly\text{-}Tyr)_2$. After fitting, a set of the parameters, namely α_1, α_2, β_1 and β_2, depending on the concentration of $(NAT)_2$, was obtained. The model predicts that a secondary plot of the ratio α_2/β_2 as a function of $1/[(NAT)_2]$ is a straight line with the intercept and slope respectively equal to $1/k_{cat(NAT)_2}^{app}$ and $K_{m(NAT)_2}^{app}/k_{cat(NAT)_2}^{app}$. Indeed a straight line was obtained (Figure 3), and the parameters [$k_{cat(NAT)_2}^{app} = 4.8 \pm 0.1\ s^{-1}$ and $K_{m(NAT)_2}^{app} = 0.55 \pm 0.05$ mM] were in good agreement with the values obtained from direct steady-state measurements of the dimerization of $(NAT)_2$ in the absence of Gly-Tyr (see above).

Peroxidases are involved in a wide number of biochemical processes. They are subject to a renewed interest because of their possible implication in different pathological processes. Among these is the involvement of the phagocytary myeloperoxidase in the formation of atherosclerotic lesions. The enzyme could mediate the oxidation of low-density lipoproteins through dityrosine formation [20] (see also [21] for a kinetic study of tyrosine oxidation by myeloperoxidase). Peroxidases could also be involved in the metabolism of L-dihydroxyphenylalanine (L-dopa) an amino acid analogue administrated in the therapy of Parkinson's disease [22]. L-dopa oxidation by peroxidases gives rise to quinones, which, in turn may form cysteinyl-dopa

© 1999 Biochemical Society

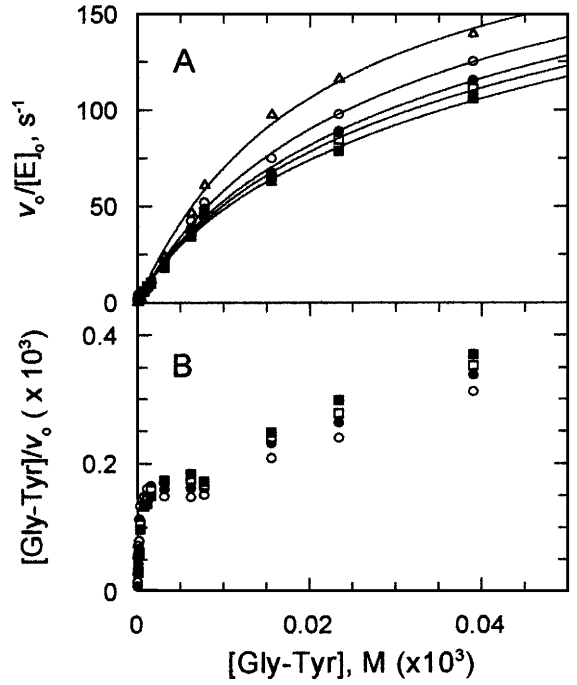

Figure 2 Effect of dimer $[(NAT)_2]$ on the initial rate of Gly-Tyr polymerization

(**A**) Initial rate of Gly-Tyr polymerization as a function of Gly-Tyr initial concentration. Experiments were carried out in 50 mM phosphate buffer, pH 8.7, containing 4 nM HRP and 100 μM H_2O_2. $(NAT)_2$ concentrations were 0 μM (△), 50 μM (○), 100 μM (●), 150 μM (□), and (■) 200μM. Continuous lines are theoretical curves corresponding to the best fit of the experimental values to eqn. (3). (**B**) Graphical representation of the Hanes equation ([Gly-Tyr]/v_0 versus [Gly-Tyr]).

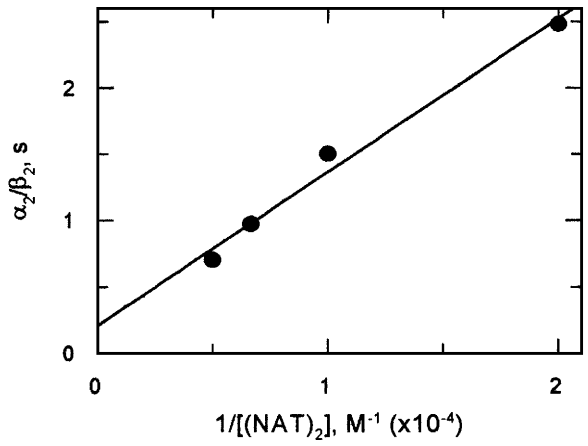

Figure 3 Secondary plot of α_2/β_2 versus the reciprocal of $(NAT)_2$ concentration

derivatives with proteins. Such altered proteins have been found in brain after dopa treatment. Speculations have been made about the potential damaging effects of long-term L-dopa therapy [23]. If several different peroxidase substrates are present in the cell at the same time, they should be processed by the enzyme simultaneously according to both their relative affinity and rate of oxidation. Thus one matter of interest in our model is that it mimics in a simplified way (only two different substrates processed at the same time) what may be found in living systems.

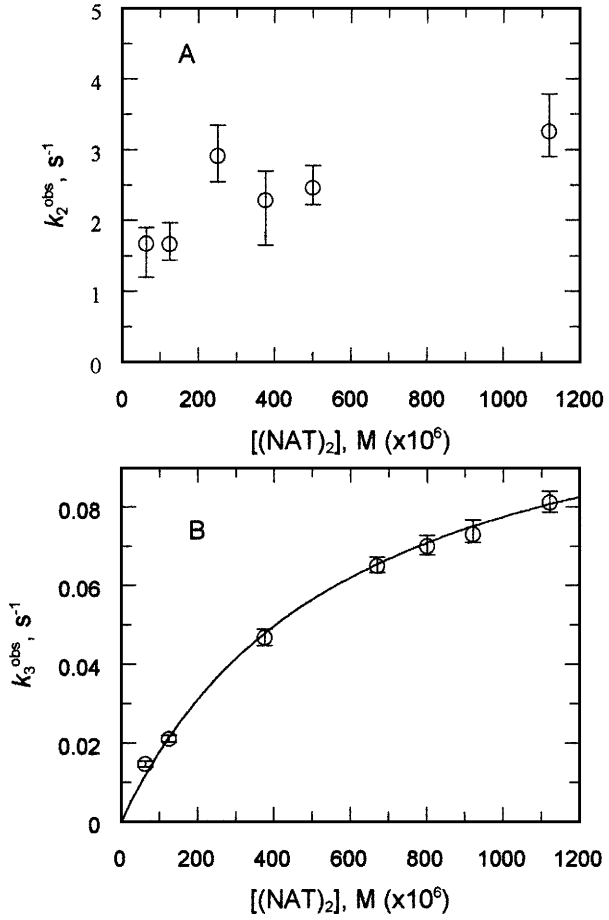

Figure 4 Plots of the pseudo-first-order rate constants versus $(NAT)_2$ concentration

(**A**) Reduction of C_I to C_{II} ($k_{I\rightarrow II}^{obs}$) and (**B**) reduction of C_{II} to the resting enzyme ($k_{II\rightarrow E}^{obs}$). Peroxidase and H_2O_2 concentrations were 5 μM in 50 mM phosphate buffer, pH 8.7, and 37 °C. The solid line shows the theoretical curve obtained after fitting the experimental data to the equation.

The system described here should provide an *in vitro* approach to evaluate the effect of drugs on the peroxidase oxidation of natural substances like tyrosine-containing peptides.

In an attempt to directly demonstrate the formation of an adsorption complex between $(NAT)_2$ and the oxidized forms of the enzyme (i.e. C_I and C_{II}), fast kinetic experiments were performed.

Determination of the pseudo-first-order rate constants of C_I and C_{II} reduction

The pseudo-first-order rate constants of the reduction of C_I and C_{II}, $k_{I\rightarrow II}^{obs}$ and $k_{II\rightarrow E}^{obs}$ respectively, were determined for several concentrations of $(NAT)_2$. If a reversible adsorption complex formed between the oxidized forms of the enzyme and $(NAT)_2$ prior to their reduction, then a plot of K^{obs} versus the donor concentration should not be linear. (In fact this would be true provided that the K_m value be in the range of the donor concentrations explored.) In the case of the reduction of C_{II} to the resting HRP, a hyperbola was obtained, and values of 0.58 ± 0.06 mM and 3.6 ± 0.2 s^{-1} were deduced for K_m^{II} and k_{cat}^{II} respectively (Figure 4B). These values were close to the parameters obtained from steady-state measurements (see above).

© 1999 Biochemical Society

This finding substantiated the hypothesis of the formation of a reversible adsorption complex between C_{II} and $(NAT)_2$ prior to C_{II} reduction. We guess that, in studies so far reported, the high values observed for $k_{I\rightarrow II}$ and $k_{II\rightarrow E}$ prevented measurements at donor concentrations high enough to observe a saturation. The 'Michaelian-like' behaviour of *p*-cresol at alkaline pH reported by Critchlow and Dunford [12] remains an intriguing case. Above pH 7, the observed rate constant for the reduction of C_{II} to the resting form of the enzyme was no longer linear with respect to *p*-cresol concentration. However, in contrast with our observations for tyrosine derivatives, no saturation was achieved as the curved part of the rate profile was followed by a linear increase of the rate over the whole range of substrate concentrations investigated. The authors concluded that a non-productive binary complex was formed between the substrate and the enzyme.

The case of tyrosine is particular. Albeit it exhibits a low $k_{II\rightarrow E}$ value, it also displays a high K_m value. Owing to solubility limitations, this feature rules out the possibility of exploring a concentration range that would allow saturation of the enzyme [24].

No saturation was observed in the case of C_I reduction to C_{II}. A plot of $k^{obs}_{I\rightarrow II}$ versus $(NAT)_2$ concentration gave a straight line which unexpectedly did not cut the ordinate at the origin of the graph (Figure 5A). One plausible explanation, albeit insufficient, might be that the adsorption complex between C_I and the electron donor display a rather low K_m, far below the range of concentration used in the experiment. The problem in exploring lower concentrations of substrates arises from the fact that it can no longer be assumed that the donor concentration in the mixing chamber during the measurement is close to the starting donor concentration. This difficulty cannot be overcome by using lower concentrations of enzyme as in such a case the signal obtained would no longer be workable. When the reduction of C_I by Gly-Tyr was examined, plots of $k^{obs}_{I\rightarrow II}$ and $k^{obs}_{II\rightarrow E}$ versus the donor concentration gave straight lines with an origin coinciding with zero concentration (Figure 5). As no saturation was obtained, we concluded that K_m values for this substrate were not accessible to measurement. The rates of reduction of the enzyme by Gly-Tyr are greater than the rates observed with $(NAT)_2$ (see Table 1). In order to explore higher donor concentrations, we tried to decrease the rates of C_I and C_{II} reduction by performing kinetic measurements at low temperature (4 °C) and low pH [24,25]. But when tests were made with donor concentrations above 500 μM, the kinetics were still too fast with respect to the response time of the apparatus.

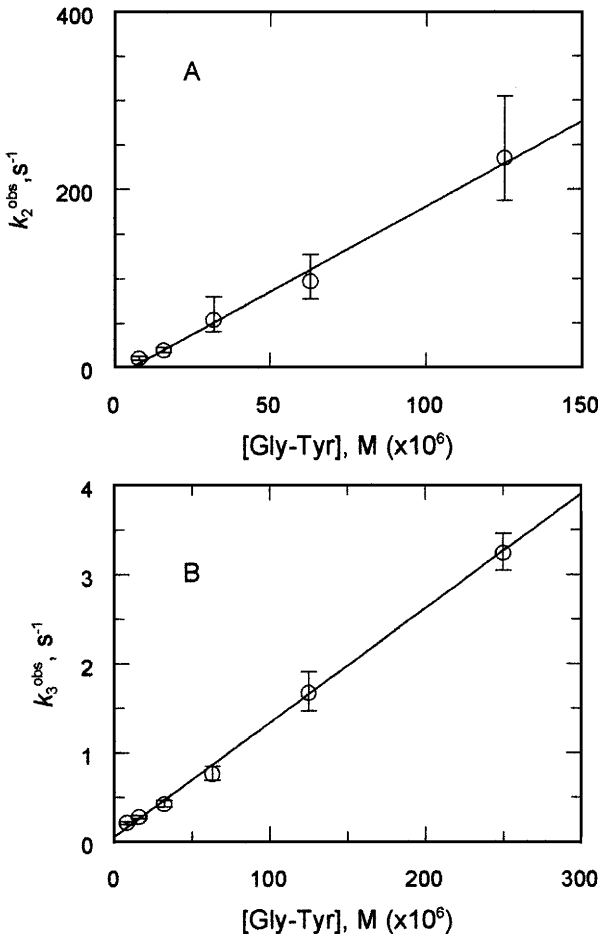

Figure 5 Plots of the pseudo-first-order rate constants (A) for the reduction of C_I to C_{II} ($k^{obs}_{I\rightarrow II}$) and (B) for the reduction of C_{II} to the resting enzyme ($k^{obs}_{II\rightarrow E}$) using Gly-Tyr as the electron donor

Peroxidase and H_2O_2 concentrations were 5 μM in 50 mM phosphate buffer, pH 8.7, and 37 °C.

Thermodynamic constant of equilibrium between $(NAT)_2$ and the resting enzyme

The binding of NAT and $(NAT)_2$ to the resting enzyme were monitored by spectroscopy (see Figure 6). Owing to the very low signal-to-noise ratio, the parameters were determined with a low accuracy. But this proved to be good enough for the purpose of comparison, as $(NAT)_2$ ($K_d = 0.7 \pm 0.1$ mM) bound ten times stronger to the HRP than did NAT ($K_d = 10 \pm 1$ mM). The thermodynamic constant of $(NAT)_2$ dissociation agreed satisfactorily both with the K^{app}_m value obtained from steady-state measurements and with K^{II}_m, the one evaluated from the stopped-flow analysis of $k^{obs}_{II\rightarrow E}$. The kinetic and thermodynamic parameters obtained through the different approaches are summarized in Table 1.

Owing to difficulties encountered when trying to experimentally observe saturation, considerations about K_m (i.e. enzyme–donor affinity) are poorly documented in the literature. Usually k_{obs} is defined as a pseudo-first-order rate of C_I or C_{II} reduction over the whole range of substrate concentration explored. This absence of saturation has been reported in the literature for many substrates. This suggested large K_m values. As a matter of fact it is frequently mentioned that HRP does not display much specificity for its various substrates. However, recently it was shown that the observed rate of C_I reduction to C_{II} could result from a combination of the rate of electron-transfer and substrate-binding thermodynamics [26]. For a given driving force, indoleacetic acids and phenols could be oxidized at very different rates. Thus it was concluded that HRP exhibits a substrate specificity with respect to the reduction of CI.

A true Michaelis constant (K^{II}_m) value of 0.6 mM was obtained from $k^{obs}_{II\rightarrow E}$. It was very close to the K^{app}_m value for the whole catalytic cycle determined from the steady-state kinetic data. We estimated this constant from eqn. (A41) of the Appendix, using $k^{II}_{cat(NAT)_2}$ and $K^{II}_{m(NAT)_2}$ values determined from the stopped-flow experiments. We failed to measure values for $k^{I}_{cat(NAT)_2}$ and $K^{I}_{m(NAT)_2}$ from the analysis of C_I reduction to C_{II}. But for $k^{I}_{cat(NAT)_2}$ ranging from 50 to 500 s^{-1} and for $K^{I}_{M(NAT)_2}$ in between 5 μM and 5 mM, the calculated K^{app}_m did not vary significantly and remained close to $K^{app}_{m(NAT)_2}$ experimental values. Thus, according to our

© 1999 Biochemical Society

Table 1 Kinetic and thermodynamic parameters for the reaction of HRP with various tyrosine derivatives

	Gly-Tyr*	$(NAT)_2$*	NAT†	L-Tyr‡
Steady-state kinetic of dimerization				
k_{cat}^{app} (s^{-1})	254	3.6	94	–
K_m^{app} (M)	24×10^{-3}	0.66×10^{-3}	5.6×10^{-3}	–
k_{cat}^{app}/K_m^{app} ($M^{-1} \cdot s^{-1}$)	1.05×10^4	5.5×10^3	1.7×10^4	–
Double-reciprocal plot $\{\alpha_2/\beta_2$ versus $1/[(NAT)_2]\}$				
k_{app}^{cat} (s^{-1})	–	4.8	–	–
K_m^{app} (M)	–	0.55×10^{-3}	–	–
k_{cat}^{app}/K_m^{app} ($M^{-1} \cdot s^{-1)}$	–	8.7×10^3	–	–
Stopped flow (HRP reduction)				
$k_{I \to II}$ ($M^{-1} \cdot s^{-1}$)	1.92×10^6	–	2.5×10^5	5.0×10^4 (5.6×10^4)
$k_{II \to E}$ ($M^{-1} \cdot s^{-1}$)	1.3×10^4	–	1.9×10^4	2×10^3 (1.1×10^3)
k_{cat}^{II} (s^{-1})	–	3.6	–	–
K_m^{II} (M)	–	0.58×10^{-3}	–	–
k_{cat}^{II}/K_m^{II} ($s^{-1} \cdot M^{-1}$)	–	6.2×10^3	–	–
K_d (M)§	–	0.7×10^{-3}	10×10^{-3}	–

* Values obtained at pH 8.5.

† Values obtained at pH 7.5 [12].

‡ Values are from [24] and [25]; because these authors performed measurements as a function of pH they were able to correct for the contribution of protons concentration; thus these are true second-order-rate-constant values; for purpose of comparison, values obtained in this laboratory at pH 7.5 are shown in parentheses.

§ Thermodynamic equilibrium constant for HRP–substrate complex formation (pH 7.5).

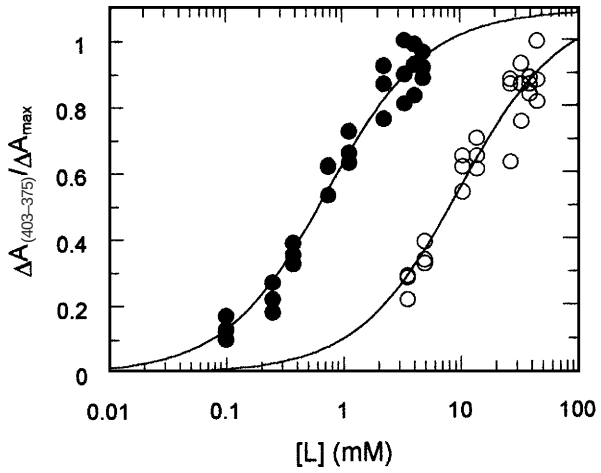

Figure 6 Titration of 7 μM native HRP with (○) NAT and (○) $(NAT)_2$ in 50 mM phosphate buffer, pH 7.5, at 25 °C

model, K_m^{app} reflects K_m^{II}. In other respects we found that the dissociation constant of the binary complex formed between the resting form of HRP and $(NAT)_2$ is on the same order of magnitude as the $K_{M(NAT)_2}^{app}$ value. This might imply that the three forms of the enzyme (E, C_I and C_{II}) display the same affinity for $(NAT)_2$. The whole catalytic cycle would proceed without major conformational changes in the enzyme. The topology of benzohydroxamic acid (BHA) in the hydrophobic pocket of a recombinant form of HRP isoenzyme C was recently published [27]. The fact that very little structural rearrangement occurs in the haem crevice in response to substrate binding supports this hypothesis. According to the structure the substrate-binding site may be divided into two domains. A hydrophobic pocket fits the aromatic ring of BHA. Beside it, the polar part of the substrate forms an extensive hydrogen-bonding network with Arg^{38}, His^{42} and Pro^{139}. The way by which the various substrates match this network might in part account for their different affinities. We previously observed that NAT is a much better substrate than L-tyrosine. These two substrates, closely related structurally, differ by the presence of a positive charge on the α-amino group of the tyrosine. A repulsive effect might occur between this group and Arg^{38}.

Our observations indicate that tyrosine dimers bind to the enzyme with a stronger affinity than monomers. BHA binds to the enzyme with a K_d of 20 μM. 2-Naphthohydroxamic acid (a two-cycle donor substrate) binds to the enzyme with an affinity ten times greater than BHA [5]. However, according to the HRP isoenzyme C–BHA crystal structure, 2-naphthohydroxamic acid cannot fit into the hydrophobic pocket of the enzyme unless Phe^{68} displays enough flexibility. It is well known that HRP can accommodate a wide range of aromatic donors, including bulky ones such as 2,2′-azinodi-(3-ethylbenzothiazoline-6-sulphonic acid). A rotation of Phe^{68} would promote the enlargement of the binding domain to a more peripheral region favouring the binding of substrates like dityrosine.

REFERENCES

1 Chance, B. (1943) J. Biol. Chem. **151**, 553–567
2 Brill, A. S. (1966) Compr. Biochem. **14**, 447–477
3 Dunford, H. B. (1991) in Peroxidases in Chemistry and Biology (Everse, J., Everse, K. E. and Gresham, M. B., eds.), vol. 2, pp. 1–24, CRC Press, Boca Raton, FL
4 Critchlow, J. E. and Dunford, H. B. (1972) J. Biol. Chem. **247**, 3714–3725
5 Schonbaum, G. R. (1973) J. Biol. Chem. **248**, 502–511
6 Adak, S., Mazumder, A. and Banerjee, R. K. (1996) Biochem. J. **314**, 985–991
7 La Mar, G. N., Hernández, G. and Ropp, J. S. (1992) Biochemistry **31**, 9158–9168
8 Childs, R. E. and Bardsley, W. G. (1975) Biochem. J. **145**, 93–103
9 Ryu, K. and Dordick, J. S. (1992) Biochemistry **31**, 2588–2598
10 Ryu, K. and Dordick, J. S. (1989) J. Am. Chem. Soc. **111**, 8026–8027
11 Job, D. and Dunford, H. B. (1978) Can. J. Biochem. **56**, 1327–1334

© 1999 Biochemical Society

12 Critchlow, J. E. and Dunford, H. B. (1972) J. Biol. Chem. **247**, 3703–3713
13 Andersen, S. O. (1966) Acta Physiol. Scand. **66** (suppl.), 263
14 Michon, T., Chenu, M., Kellershon, N., Desmadril, M. and Guéguen, J. (1997) Biochemistry **36**, 8504–8513
15 Malencik, D. A., Sprouse, J. F., Swanson, C. A. and Anderson, S. R. (1996) Anal. Biochem. **242**, 202–213
16 Schejter, A., Lanir, A. and Epstein, N. (1976) Arch. Biochem. Biophys. **174**, 36–44
17 Marquardt, D. W. (1963) J. Soc. Ind. Appl. Math. **11**, 431–441
18 Spendley, W., Hext, G. R. and Himsworth, F. R. (1962) Technometrics **4**, 441–461
19 Cornish-Bowden, A. (1979) in Fundamentals of Enzyme Kinetics, pp. 26–27, Butterworth and Co. Ltd., Borough Green, Sevenoaks
20 Savenkova, M. I., Mueller, D. M. and Heinecke, J. W. (1994) J. Biol. Chem. **269**, 20394–20400
21 Marquez, A. M. and Dunford, H. B. (1995) J. Biol. Chem. **270**, 30434–30440
22 Graham, D. (1978) Mol. Pharmacol. **14**, 633–643
23 Fornsted, B., Rosengren, E. and Carlsson, A. (1986) Neuropharmacology **25**, 451–454
24 Ralston, I. M. and Dunford, H. B. (1980) Can. J. Biochem. **58**, 1270–1276
25 Ralston, I. M. and Dunford, H. B. (1978) Can. J. Biochem. **56**, 1115–1119
26 Candeias, L. P., Folkes, L. K. and Wardman, P. (1997) Biochemistry **36**, 7081–7085
27 Henriksen, A., Schuller, D. J., Meno, K., Welinder, K. G., Smith, A. T. and Gajhede, M. (1998) Biochemistry **37**, 8054–8060

APPENDIX

Reference should be made to Scheme 1 of the main paper. The Michaelis constants for each step are defined as follows:

$$K_m^{IA} = \frac{k_{-2} + k_{cat}^{IA}}{k_2} \quad (A1)$$

$$K_m^{IB} = \frac{k_{-3} + k_{cat}^{IB}}{k_3} \quad (A2)$$

$$K_m^{IIA} = \frac{k_{-4} + k_{cat}^{IIA}}{k_4} \quad (A3)$$

$$K_m^{IIB} = \frac{k_{-5} + k_{cat}^{IIB}}{k_5} \quad (A4)$$

The steady-state rate equations for the variation of the enzymic species are:

$$\frac{dE}{dt} = k_{cat}^{IIA} \cdot C_{II}A + k_{cat}^{IIB} \cdot C_{II}B - k_1 \cdot S \cdot E = 0 \quad (A5)$$

$$\frac{dC_I}{dt} = k_{-3} \cdot C_I B + k_{-2} \cdot C_I A + k_1 \cdot S \cdot E - (k_2 \cdot A + k_3 \cdot B) \cdot C_I = 0 \quad (A6)$$

$$\frac{dC_{II}}{dt} = k_{cat}^{IA} \cdot C_I A + k_{cat}^{IB} C_I B + k_{-4} C_{II} A + k_{-5} C_{II} B - (k_4 A + k_5 B) \cdot C_{II} = 0 \quad (A7)$$

$$\frac{dC_I A}{dt} = k_2 \cdot C_I \cdot A - (k_{cat}^{IA} + k_{-2}) \cdot C_I A = 0 \quad (A8)$$

$$\frac{dC_I B}{dt} = k_3 \cdot C_I \cdot B - (k_{cat}^{IB} + k_{-3}) \cdot C_I B = 0 \quad (A9)$$

$$\frac{dC_{II} A}{dt} = k_4 \cdot C_{II} \cdot A - (k_{cat}^{IIA} + k_{-4}) \cdot C_{II} A = 0 \quad (A10)$$

$$\frac{dC_{II} B}{dt} = k_5 \cdot C_{II} \cdot B - (k_{cat}^{IIB} + k_{-5}) \cdot C_{II} B = 0 \quad (A11)$$

with S being H_2O_2 concentration.
The mass conservation is:

$$E_0 = E + C_I + C_I A + C_I B + C_{II} + C_{II} A + C_{II} B \quad (A12)$$

The steady-state initial rate of free radical formation is:

$$v_0 = k_{cat}^{IA} \cdot C_I A + k_{cat}^{IB} \cdot C_I B + k_{cat}^{IIA} \cdot C_{II} A + k_{cat}^{IIB} \cdot C_{II} B \quad (A13)$$

$$C_I A = \frac{A}{K_m^{IA}} \cdot C_I \quad (A14)$$

and in the same way using eqns. (A2) and (A9)

$$C_I B = \frac{B}{K_m^{IB}} \cdot C_I \quad (A15)$$

using eqns. (A3) and (A10)

$$C_{II} A = \frac{A}{K_m^{IIA}} \cdot C_{II} \quad (A16)$$

with eqns. (A4) and (A11)

$$C_{II} B = \frac{B}{K_m^{IIB}} \cdot C_{II} \quad (A17)$$

Let us consider eqn. (A7). Using eqns. (A14)–(A17) we can replace $C_I A$, $C_I B$, $C_{II} A$ and $C_{II} B$ with their expression as functions of C_I and C_{II}:

$$\left(\frac{k_{cat}^{IA}}{K_m^{IA}} \cdot A + \frac{k_{cat}^{IB}}{K_m^{IB}} \cdot B\right) \cdot C_I = \left(\frac{k_4 \cdot K_m^{IIA} - k_{-4}}{K_m^{IIA}} \cdot A + \frac{k_5 \cdot K_m^{IIB} - k_{-5}}{K_m^{IIB}} \cdot B\right) \cdot C_{II}$$

and referring to eqns. (A3) and (A4) we get:

$$\Phi_{(A,B)} \cdot C_I = \Psi_{(A,B)} \cdot C_{II} \quad (A18)$$

with

$$\Phi_{(A,B)} = \frac{k_{cat}^{IA}}{K_m^{IA}} \cdot A + \frac{k_{cat}^{IB}}{K_m^{IB}} \cdot B \quad (A19)$$

$$\Psi_{(A,B)} = \frac{k_{cat}^{IIA}}{K_m^{IIA}} \cdot A + \frac{k_{cat}^{IIB}}{K_m^{IIB}} \cdot B \quad (A20)$$

It is convenient to express all the enzyme species as functions of C_I. Hence from eqn. (A18):

$$C_{II} = \frac{\Phi_{(A,B)}}{\Psi_{(A,B)}} \cdot C_I \quad (A21)$$

Eqns. (A16) and (A17) become:

$$C_{II} A = \frac{A}{K_m^{IIA}} \cdot \frac{\Phi_{(A,B)}}{\Psi_{(A,B)}} \cdot C_I \quad (A22)$$

$$C_{II} B = \frac{B}{K_m^{IIB}} \cdot \frac{\Phi_{(A,B)}}{\Psi_{(A,B)}} \cdot C_I \quad (A23)$$

Considering eqn. (A5) and using eqns. (A16)–(A18) we can express E as a function of C_I, A and B as follows:

$$k_1 \cdot S \cdot E = \left(\frac{k_{cat}^{IIA}}{K_m^{IIA}} \cdot A + \frac{k_{cat}^{IIB}}{K_m^{IIB}} \cdot B\right) \cdot \frac{\Phi_{(A,B)}}{\Psi_{(A,B)}} \cdot C_I \quad (A24)$$

© 1999 Biochemical Society

Rearranging:

$$E = \frac{1}{k_1 \cdot S} \cdot \Phi_{(A,B)} \cdot C_I \tag{A25}$$

Replacing every species with its expression as a function of C_I we obtain:

$$E_0 = \left[\frac{\Phi_{(A,B)}}{k_1 \cdot S} + 1 + \frac{A}{K_m^{IA}} + \frac{B}{K_m^{IB}} + \frac{\Phi_{(A,B)}}{\Psi_{(A,B)}} \cdot \left(1 + \frac{A}{K_m^{IIA}} + \frac{B}{K_m^{IIB}}\right)\right] \times C_I = H_{(A,B)} \cdot C_I \tag{A26}$$

Hence:

$$C_I = \frac{E_0}{H_{(A,B)}} \tag{A27}$$

Expression of v_0 as a function of S, A and B

Starting from eqn. (A13) and using eqns. (A14), (A15), (A22) and (A23) we can write:

$$v_0 = 2 \cdot \Phi_{(A,B)} \cdot C_I \tag{A28}$$

Replacing C_I according to eqn. (A27)

$$\frac{v_0}{E_0} = \frac{2 \cdot \Phi_{(A,B)}}{H_{(A,B)}} \tag{A29}$$

Rearranging the rate equation with respect to A and keeping the concentration of B (B) constant, an expression of the initial rate of free-radical formation as a ratio of two polynomials with respect to A is obtained:

$$\frac{v_0}{[E]_0} = 2 \times \frac{[A]^2 + \beta_1[A] + \beta_2}{\left(\frac{1}{k_{cat}^A} + \frac{1}{k_1 S}\right)[A]^2 + \left(\alpha_1 + \frac{\beta_1}{k_1 S}\right)[A] + \left(\alpha_2 + \frac{\beta_2}{k_1 S}\right)} \tag{A30}$$

$$\alpha_1 = a_1[B] + K_{m_a}^{app}/k_{cat_A}^{app} \tag{A31}$$

with

$$a_1 = \frac{1}{k_{cat}^{IA} \cdot K_{cat}^{IIA}} \left(\frac{(k_{cat}^{IIA} + k_{cat}^{IB}) \cdot K_m^{IA}}{K_m^{IB}} + \frac{(k_{cat}^{IA} + k_{cat}^{IIB}) \cdot K_m^{IA}}{K_m^{IIB}}\right) \tag{A32}$$

$$\alpha_2 = a_2[B] + a_3[B]^2 \tag{A33}$$

Received 20 January; accepted 17 February 1999

with

$$\left.\begin{aligned} a_2 &= \frac{K_m^{IA} \cdot K_m^{IIA}}{k_{cat}^{IA} \cdot k_{cat}^{IIA} \cdot K_m^{IB} \cdot K_m^{IIB}} (k_{cat}^{IB} \cdot K_m^{IIB} + k_{cat}^{IIB} \cdot K_m^{IB}) \\ a_3 &= \frac{K_m^{IA} \cdot K_m^{IIA}}{k_{cat}^{IA} \cdot k_{cat}^{IIA} \cdot K_m^{IB} \cdot K_m^{IIB}} (k_{cat}^{IB} + k_{cat}^{IIB}) \end{aligned}\right\} \tag{A34}$$

and

$$\beta_1 = b_1[B] \tag{A35}$$

with

$$b_1 = \frac{k_{cat}^{IB} \cdot K_m^{IA}}{k_{cat}^{IA} \cdot K_m^{IB}} + \frac{k_{cat}^{IIB} \cdot K_m^{IIA}}{k_{cat}^{IIA} \cdot K_m^{IIB}} \tag{A36}$$

$$\beta_2 = b_2[B]^2 \tag{A37}$$

with

$$b_2 = \frac{k_{cat}^{IB} \cdot k_{cat}^{IIB} \cdot K_m^{IA} \cdot K_m^{IIA}}{k_{cat}^{IA} \cdot k_{cat}^{IIA} \cdot K_m^{IB} \cdot K_m^{IIB}} \tag{A38}$$

The model is symmetrical, and the forms of the equations are the same when written with respect to B, keeping A constant. However it is noteworthy that the rates of free-radical formation through both pathways are not additive. There is a partitioning of the enzyme between its complexes with A and B (i.e. $C_I A$, $C_{II} A$, $C_I B$ and $C_{II} B$) according to their relative affinities.

In the absence of the second substrate ([B] = 0 for example) eqn. (A30) is simplified to

$$\frac{v_0}{[E]_0} = 2 \cdot \frac{k_{cat}^{app} \cdot k_1 \cdot S}{(k_{cat_a}^{app} + k_1 \cdot S)} \cdot \frac{[A]}{K_{m_a}^{app} \cdot \frac{k_1 \cdot S}{(k_{cat_A}^{app} + k_1 \cdot S)} + [A]} \tag{A39}$$

and the apparent kinetic parameters directly accessible from steady-state measurements are:

$$k_{cat_A}^{app} = \frac{k_1 \cdot S \cdot k_{cat}^{IA} \cdot k_{cat}^{IIA}}{k_1 \cdot S \cdot (k_{cat}^{IA} + k_{cat}^{IIA}) + k_{cat}^{IA} \cdot k_{cat}^{IIA}} \tag{A40}$$

$$K_{m_A}^{app} = \frac{k_1 \cdot S \cdot (K_m^{IA} \cdot k_{cat}^{IIA} + K_m^{IIA} \cdot k_{cat}^{IA})}{k_1 \cdot S \cdot (k_{cat}^{IA} + k_{cat}^{IIA}) + k_{cat}^{IA} \cdot k_{cat}^{IIA}} \tag{A41}$$

$$\frac{k_{cat_A}^{app}}{K_{m_A}^{app}} = \frac{k_{cat}^{IA} \cdot k_{cat}^{IIA}}{(K_m^{IA} \cdot k_{cat}^{IIA} + K_m^{IIA} \cdot k_{cat}^{IA})} \tag{A42}$$

It may be shown that a secondary plot of α_2/β_2 (i.e. eqn. A33/eqn. A37) versus 1/[B] gives a straight line with slope and intercept equal to $K_{m_B}^{app}/k_{cat_B}^{app}$ and $1/k_{cat_B}^{app}$ respectively.

© 1999 Biochemical Society